An experimental study on the formation of polycyclic aromatic hydrocarbons in laminar coflow non-premixed methane/air flames doped with four isomeric butanols

Jin, Hanfeng; Wang, Yizun; Zhang, Kuiwen; Guo, Hongsheng; Qi, Fei

Publisher's version / Version de l'éditeur:
https://doi.org/10.1016/j.proci.2012.05.107
Proceedings of the Combustion Institute, 34, 1, pp. 779-786, 2012-06-23

An experimental study on the formation of polycyclic aromatic hydrocarbons in laminar coflow non-premixed methane/air flames doped with four isomeric butanols

Hanfeng Jin[1], Yizun Wang[1], Kuiwen Zhang[2], Hongsheng Guo[3], Fei Qi[1,2*]

[1] *State Key Laboratory of Fire Science, University of Science and Technology of China, Hefei, Anhui 230026, P. R. China*

[2] *National Synchrotron Radiation Laboratory, University of Science and Technology of China, Hefei, Anhui 230026, P. R. China*

[3] *National Research Council Canada, 1200 Montreal Road, Building M-9, Ottawa, Ontario, Canada K1A 0R6*

Abstract: Experimental measurements were conducted for temperatures and mole fractions of C1-C16 combustion intermediates in laminar coflow non-premixed methane/air flames doped with 3.9% (volume based) of 1-butanol, 2-butanol, *iso*-butanol and *tert*-butanol, respectively. Synchrotron vacuum ultraviolet photoionization mass spectrometry (SVUV-PIMS) technique was utilized in the measurements of species mole fractions. The results show that the variant molecular structures of butyl alcohols have led to different efficiencies in the formation of polycyclic aromatic hydrocarbons (PAHs) that may cause the variations in sooting tendency. Detailed species information suggests that the presence of allene and propyne promotes benzene formation through the C_3H_3 + C_3H_4 reactions and consequently PAH formation through the additions of C2 and C3 species to benzyl or phenyl radicals. As a matter of fact, PAH emissions from 1-butanol doped flame are the lowest among the four investigated flames, because 1-butanol mainly decomposes to ethylene and oxygenates rather than C3 hydrocarbon species. Meanwhile, *tert*-butanol doped flame generates the largest quantities of allene and propyne among the four flames and therefore is the sootiest one.

Keywords: non-premixed diffusion flame; butanol; synchrotron VUV photoionization mass

* Corresponding author. E-mail: fqi@ustc.edu.cn, Fax: +86-551-5141078, Tel: +86-551-3602125.

spectrometry; benzene and PAH formation

1. Introduction

Fossil fuels are still the dominant energy resources of transportation worldwide. However, climate change and limited fossil supply are incentive to search for cleaner and sustainable energy sources [1]. Biofuels are widely discussed as sustainable transportation fuels, because they are renewable and the application of them can reduce net greenhouse gas emissions. Butanol is a biofuel that has been considered as a suitable additive and/or alternative to gasoline and diesel, even better than ethanol. The energy density of butanol (29.2 MJ/L) is about 90% of gasoline's, higher than ethanol [2,3]. It can replace gasoline liter-for-liter in spark ignition engines [4] and be blended with a fraction of 40% in diesel engines. It is more hydrophobic and can be shipped by the existing fuel pipelines, while ethanol must be transported via truck and rail. Recently, Dupont and British Petroleum have been converting a British Sugars ethanol plant into a 1-butanol pilot plant [5,6]. Thus, butanol receives more and more attention in combustion community recently.

Engine performances of butanol-gasoline blend were carried out before detailed combustion kinetic mechanism investigation [7-12]. Several experimental studies focusing on the combustion characteristics of butyl alcohols have also been published by presenting a wealth of combustion data obtained in shock-tubes [2,13-16], flow reactors [17,18], jet-stirred reactors [2,19-23] and flames [17,22,24-28]. Coupled to these experiments, kinetic modeling studies have been performed, which resulted in a detailed description of the high-temperature fuel chemistry [2,13,17,19,22,27].

The decomposition process for butyl alcohols was studied by McEnally and Pfefferle [24] by using laminar coflow methane/air flames doped with four butanol isomers, separately. In their experiments, stable flame species concentrations were primarily measured with a custom-built 118 nm (10.5 eV) single-photon photoionization time-of-flight mass spectrometer. Species whose ionization energies exceed 10.5 eV (such as C_2H_2, CH_4, and CH_2O) were measured with an electron-impact quadrupole mass spectrometer. About 30 flame intermediates were detected in their experiments. However, isomers of combustion intermediates were not identified. Their main conclusion was that unimolecular dissociation, including C-C bond fission and dehydration reactions,

is the dominant fuel consumption pathway for all four butanol isomers. Yang et al. [26] studied fuel-rich premixed laminar butanol flames at low pressure to identify the intermediates. Recently Oßwald et al. [25] reported quantitative results of an experimental study on the four isomeric butanol premixed flames at low pressure by both EI and synchrotron-based PI mass spectrometry. A study on opposed-flow diffusion flames were carried out by Sarathy et al. [22] and Grana et al. [27] to investigate the combustion chemistry of butyl alcohols. Major species and most of the important fuel decomposition intermediates besides acetone and unsaturated alcohols were detected in their experiments. Sarathy et al. observed that in 1-butanol flame, H-abstraction followed by β-scission was the major pathway for 1-butanol consumption, while Grana et al. found that in 1-butanol and *iso*-butanol flames, the flame structures and overall combustion characteristics of butyl alcohols were similar.

Although the decomposition pathways of four butanol isomers have been widely discussed in previous experiments and mechanisms mentioned above, not enough attention has been paid to the formation process of benzene and polycyclic aromatic hydrocarbons (PAHs). Both models developed by Moss et al. [2] and Black et al. [13] do not include pathways of benzene formation. The mechanisms of Sarathy et al. [22] and Harper et al. [17] can poorly estimate the benzene yield. Grana et al. [27] did not predict the benzene profile in their works. McEnally et al. [24] and Oßwald et al. [25] presented benzene profiles at the end of their literatures, but there were lack of discussions in detail.

In present study, the laminar coflow non-premixed methane/air flames doped by four butanol isomers, respectively, are investigated at atmospheric pressure. The synchrotron-based vacuum ultraviolet photoionization mass spectrometry (SVUV-PIMS) technique was used to identify combustion intermediates and final products, including PAHs. Stable C1-C16 hydrocarbons and oxygenates were measured and identified to understand the combustion chemistry, especially in PAH formation. Their mole fraction profiles are also presented in this paper for further modeling validation.

2. Experimental methods

The experiments were carried out at National Synchrotron Radiation Laboratory in Hefei, China.

Synchrotron radiation from an undulator beamline of the 800 MeV electron storage ring is monochromarized with a 1 m Seya-Namioka monochromator equipped with a 1500 grooves/mm laminar grating. The energy resolving power (E/ΔE) is about 1000.

The schematic experimental set up is shown in Fig. 1. The instrument is composed of a laminar coflow non-premixed burner, a differentially pumped chamber with a molecular-beam sampling system and an ionization chamber with a home-made reflectron time-of-flight mass spectrometer (RTOF-MS). Atmospheric-pressure coflow non-premixed flames are generated by a burner with a 102 mm inner-diameter air tube. The mixture of fuel (CH_4 and C_4H_9OH), dilute gas N_2 and calibration gas Ar flows through a 10 mm inner-diameter stainless steel fuel tube that is located at the center of the air tube. Air flows through the annular region between fuel and air tubes. Thickness of the fuel inner tube is 1 mm. The metal foam and glass beads were used in the air tube to reduce the instability of the air flow. The burner was fixed on a 2D-step-motor-locator to control the gas sampling position along the flame height and radial direction.

A quartz probe with an orifice of about 150 μm in diameter was used to sample the flame. Molecular beam is formed after the sampling gases pass through a nickel skimmer into ionization region. The molecules are ionized by synchrotron VUV light which is crossed with molecular beam in the ionization region. The ions are then detected by the RTOF-MS, which has been described in previous report of low-pressure premixed flames [29].

Species along the central axis (marked as Z-axis in Fig. 1) were profiled. A major problem in the measurement was that the sampling probe could be easily blocked by soot at the center of flame within 10 seconds. Fortunately, the soot can be burned out quickly in the stoichiometric reaction zone at the edge of the flame. Thus, for a given position and photon energy, the probe tip was moved to the stoichiometric reaction zone to burn out the soot after taking one spectrum at the central axis. Usually, 25 cycles were repeated to stack up enough signals for one valid mass spectrum. The region at the bottom of the flame could not be sampled because of the shape limit of sampling probe. Mass spectra were taken at the photon energies of 16.64, 15.20, 14.50, 12.00, 11.00, 10.00, and 9.50 eV to perform near threshold photoionization measurement and calculate the mole fractions of isomers.

Flame temperature profiles along Z-axis were measured by Pt-6%Rh/Pt-30%Rh thermocouple, which is 0.1 mm in diameter, and coated with Y_2O_3-BeO anticatalytic ceramic to avoid catalytic effects [30]. The uncertainty of the temperature measurement is about ±50 K. The gas temperature at the sooting region in the flame could be underestimated by about 120 K due to the soot attached to the thermocouples.

Flame conditions are presented in Table 1. The mole fractions in the fuel mixture are 25.46% for CH_4, 69.70% for N_2, 0.93% for Ar and 3.90% for the dopant. Flow rates of the gas reagents were controlled by MKS mass flow controllers, while the flow rates of liquid fuels injected into the vaporizer were controlled by a liquid chromatographic pump. In order to avoid the liquefaction of butanol, the vaporizer temperature was kept 30 K higher than the boiling point of each butanol isomer, and the temperature of fuel mixture was kept at 493 K during the experiment.

An approximate method proposed by Cool et al. [31] was used in the data reduction. The relation between the ion signal intensity and mole fraction of species *i* is described by Eq. (1),

$$S_i(T) = CX_i(T)D_i\sigma_i(E)\Phi_p(E)F(k,T,P) \quad (1)$$

where, C is a constant of proportionality; $S_i(T)$ is the ion signal intensity; T and $X_i(T)$ are the local flame temperature and species mole fraction, respectively, at the sampling position; $\sigma_i(E)$ is the photoionization cross-section at the photon energy E; D_i is the mass discrimination factor for species i; $\Phi_p(E)$ is the photon flux; and $F(k,T,P)$ is an empirical instrumental sampling function that relates the molecular beam molar density at the ionization region to the flame pressure P and local temperature T. Therefore, the mole fraction of a chosen species sampled at any position could be calculated by Eq. (2) and Eq. (3),

$$X_i(T) = X_i(T_0)\times[S_i(T)/S_i(T_0)]/[F(k,T,P)/F(k,T_0,P)] = X_i(T_0)\times[S_i(T)/S_i(T_0)]/FKT(T,T_0) \quad (2)$$

$$FKT(T,T_0) = F(k,T,P)/F(k,T_0,P) \quad (3)$$

And $FKT(T, T_0)$ is defined as a normalized sampling function. Since the mole fraction of Ar in the inlet fuel mixture is the same as that in the air, its diffusion effect is negligible. Therefore, $FKT(T,T_0)$ can be given by Eq. (4) by using the measurements of $S_{Ar}(T)/S_{Ar}(T_0)$ of Ar, where T_0 refers to the first sampling position at 5.5 mm above the burner exit and T_F refers to the final sampling position at 71.5

mm above the burner exit.

$$FKT(T,T_0) = [S_{Ar}(T)/S_{Ar}(T_0)]/\{X_{Ar}(T_F)/X_{Ar}(T_0) + [S_{Ar}(T)/S_{Ar}(T_0) - S_{Ar}(T_F)/S_{Ar}(T_0)] \times [1 - X_{Ar}(T_F)/X_{Ar}(T_0)]/[1 - S_{Ar}(T_F)/S_{Ar}(T_0)]\} \quad (4)$$

For major flame species including CH_4, C_4H_9OH, H_2, H_2O, CO, CO_2, O_2, N_2 and Ar, the mole fractions at T_0 and T_F were calculated by solving Eqs. (5) and (6), and then the mole fractions at other positions could be given from Eq. (2). Cold flow measurements of binary mixtures (such as CO/Ar) were used to determine the ratio of photoionization cross sections and mass discrimination factors ($[D_{CO}\sigma_{CO}(E)]/[D_{Ar}\sigma_{Ar}(E)]$).

$$X_i(T) = X_{Ar}(T) \times [S_i(T)/S_{Ar}(T)] \times [D_i\sigma_i(E)]/[D_{Ar}\sigma_{Ar}(E)] \quad (5)$$

$$\sum X_i(T) = 1 \quad (6)$$

For intermediate species *i*, the mole fractions were evaluated by Eq. (7) from the known mole fractions of species *j*, in which absolute or estimated photoionization cross sections are used.

$$X_i(T) = X_j(T) \times [S_i(T)/S_j(T)] \times [D_i\sigma_i(E)]/[D_j\sigma_j(E)] \quad (7)$$

The mole fraction uncertainty is in about 20% for major species, about 50% for intermediate species with known photoionization cross sections and a factor of 2 for intermediate species with estimated photoionization cross sections.

3. Result and discussion

3.1. Flame temperature

The centerline flame temperatures (T_f) and the benzene mole fractions in the methane flames doped with butanol isomers are shown as a function of the height above burner surface (Z) in the bottom right of Fig. 1. The temperature near the burner surface is about 500 K, since the fuel/gas mixture has been preheated. The temperature increases rapidly while Z increases and peaks at about Z = 60 mm. Then the flame temperature starts to decrease with further increasing of Z. The difference among the temperature profiles of the four butanol doped flames seems negligible along the whole centerline and the maximum centerline temperature is at about Z = 60 mm for all four flames.

However, the mole fractions of intermediate species are quite different. It is noted from Fig. 1 that the maximum mole fractions of benzene in the four flames are significantly different, with that in the

tert-butanol doped flame being almost twice of those in the 1-butanol and 2-butanol doped flames. Since benzene appears in the region of Z = 15 - 56 mm where the difference of centerline temperature among the four flames is less than 50 K and the mole fraction peaks at the same position (Z = 38 mm) for all four flames, the differences in the mole fraction profiles of benzene among the four flames are caused by chemical effects of the fuels, rather than thermal or resident time effects.

3.2 Fuel decomposition

Figure 2 shows the measured centerline mole fraction profiles of C2-C4 intermediates as a function of height above burner in the four isomeric butanol doped flames. The decomposition processes of four butanol isomers have been discussed frequently in literatures [2,19,20,22-25]. Since the oxygenated free radicals could rarely diffuse from near stoichiometric zone to the centerline area of the flame, the pathways of fuel decomposition in the coflow flames are quite similar to pyrolysis circumstance. In the primary fuel consumption zone, carbon bond fission and dehydration reaction still dominate the consumption of butanol isomers [17,24]. Maybe H-atom abstraction is also important in the area slightly above the exit of the burner because of two reasons: (1) low gas temperature in the area reduces the rate constant of unimolecular reactions, and (2) the decomposition of methane yields large amount of H-atom.

Formaldehyde, acetaldehyde, ethenol, and ethylene have high concentrations in the 1-butanol doped flame, as shown in Fig. 2. These are primary decomposition products of fuel. C-C bond fission at different positions of 1-butanol would produce the following free radicals: $CH_3CH_2CH_2$, CH_2OH, CH_3CH_2, CH_2CH_2OH, $CH_2CH_2CH_2OH$. Especially, the rupture of the α-C-C bond that is the most favorable reaction in the 1-butanol doped flame yields radicals $CH_3CH_2CH_2$ and CH_2OH [32]. Ethylene, formaldehyde, and ethenol are formed from the further β-fission of these radicals. Since ethylene is the main product of $CH_3CH_2CH_2$, CH_3CH_2 and $CH_2CH_2CH_2OH$, its mole fraction in the 1-butanol doped flame is the highest among the four isomeric butanol doped flames.

In the 2-butanol doped flame, C-C bond fission of 2-butanol would form radicals CH_3CH_2CHOH, CH_3CHOH, CH_3CH_2, and $CH_2CH(CH_3)OH$. The further β-fission of them would easily form ethenol, acetaldehyde, ethylene and acetone, respectively. The high concentrations of

these species confirm that C-C bond fission dominates the consumption of 2-butanol in this study, as shown in Fig. 2. Dehydration reaction occurs more easily to form more C_4H_8 (2-butene) in fuel decomposition process in the 2-butanol doped flame than the 1-butanol doped flame. The mole fractions of 1,3-butadiene in the 2-butanol doped flame is the highest among the four flames, because 1,3-butadiene is more easier to be produced by 2-butene than other C_4H_8 isomers [33].

In the *iso*-butanol doped flame, both propene and formaldehyde have high mole fractions, which can be explained by the C-C bond fission of *iso*-butanol. CH_3CHCH_3, CH_2OH and CH_3CHCH_2OH radicals that are yielded from the unimolecular decomposition of *iso*-butanol undergo β-fission to form propene and formaldehyde. Part of the β-fission reaction of CH_3CHCH_2OH radical forms the largest amount of propenol among the four flames. This clearly suggests that unimolecular carbon bond fission controls the butanol decomposition chemistry in the current experimental condition. The observed mole fractions of formaldehyde in the *iso*-butanol and 1-butanol doped flames are almost same, as shown in Fig. 2a. This is because R-CH_2OH structure (R refers to any alkyl) that would easily decompose to CH_2OH radical to form formaldehyde exists in both *iso*- and 1- butanols. The mole fraction of butene (*iso*-butene) in the *iso*-butanol doped flame is more than that (1-butene) in the 1-butanol doped flame. It is also a result of the dehydration reaction of *iso*-butanol.

In the *tert*-butanol doped flame, the mole fractions of *iso*-butene and acetone are the highest among the four isomeric butanol doped flames. This can be explained as following. Dehydration reaction would be very easy to happen for *tert*-butanol, since there are three methyl groups. It consumes most of the *tert*-butanol while C-C bond fission consumes the rest. C-C bond fission produces large amount of acetone via the β-fission of $CH_3C(CH_3)OH$ radical, as shown in Fig. 2d. The mole fraction of 1,3-butadiene is low in contrast to the high butene mole fraction in the *tert*-butanol doped flame. The transformation from *iso*-butene to 1,3-butadiene may occurs by the reaction sequence i-$C_4H_8 \rightarrow i$-$C_4H_7 \rightarrow CH_2{=}CHCHCH_3 \rightarrow C_4H_6$. This has been proposed in the previous work of Yasunaga's and Zhang's *iso*-butene models [33,34]. Because of the low efficiency of the isomerization reaction between i-C_4H_7 and $CH_2{=}CHCHCH_3$ radicals, 1,3-butadiene would be

hard to form in this flame. The mole fraction of butene (*iso*-butene) in the *iso*-butanol doped flame is similar to that (2-butene) in the 2-butanol doped flame. Hence, there is less 1,3-butadiene in the former flame. Most *i*-C_4H_7 radical that yielded from *iso*-butene decomposition is going to form allene and propyne through β-fission.

3.3 Hydrocarbon growth

The benzene mole fraction in the four isomeric butanol doped flames are in the order of 1-butanol < 2-butanol < *iso*-butanol < *tert*-butanol in this study, as shown in Fig. 1. Similar result has been reported in the premixed butanol flames by Oßwald et al. [25], although there is more oxygenic radical in the premixed flames. Figure 3 shows that the magnitudes of the mole fractions of all detected aromatics also obey the order that has been observed for benzene in the four flames. It shows certain regularity related to the degree of branching, and suggests that benzene formation is the rate-limiting step for PAH formation.

Mole fractions of ethylene, acetylene, allene, propyne, 1,3-butadiene, and vinylacetylene, which are considered as important benzene precursors, were measured in this work. However, the mole fractions of free radicals (C_4H_5, C_4H_3, C_3H_3, C_2H_3, CH_3 et al.) are too low to be detected in the atmosphere pressure flames. Comparing mole fractions of these C3 and C4 species among the four butanol doped flames, only the order for the mole fractions of allene and propyne is the same as that of benzene. Since propargyl radical forms mainly through the H-abstraction and H-elimination of allene and propyne, it suggests that the addition of propargyl radical on allene and propyne may dominate the benzene formation process in all the butanol doped flames.

However, the contributions of other benzene formation pathways also need to be considered. In the *iso*-butanol doped flame, high mole fraction of propene indicates that there is plenty of C_3H_5 radical. Thus, the radical recombination reaction between allyl and propargyl ($C_3H_5 + C_3H_3 \leftrightarrow C_6H_6 + 2H$) may be also of great contribution to benzene formation. In the 1-butanol doped flame, due to the highest concentration of ethylene, C_2H_3 radical could easily be produced from C_2H_4. Therefore, the addition of C_2H_3 radical to vinylacetylene ($C_4H_4 + C_2H_3 \leftrightarrow C_6H_6 + H$) may be more important in this flame. In the 2-butanol doped flame, because of the high mole fraction of 1,3-butadiene, C_4H_5

that formed from 1,3-butadiene could react through $C_4H_5 + C_2H_2 \leftrightarrow C_6H_6 + H$, serving as a complementary pathway of benzene formation.

Monocyclic aromatic hydrocarbons (MAHs), including toluene, styrene, and phenylacetylene, are proposed to form through the addition reactions of methyl and C2 species on phenyl and benzene. Toluene formation easily occurs by the recombination of phenyl (or benzene) and methyl radical, because of the high mole fractions of methyl radical in these methane flames. According to the experimental results in Figs. 3b and 3c, mole fraction of styrene is smaller than that of phenylacetylene, and ethylbenzene could be hardly detected. Therefore, the pathway of $C_6H_5 + C_2H_2 \leftrightarrow C_6H_5CCH + H$ and $C_6H_6 + C_2H \leftrightarrow C_6H_5CCH + H$ may dominate the phenylacetylene formation process. Similar pathway could be built up in the formation of styrene: $C_6H_5 + C_2H_4 \leftrightarrow C_6H_5CHCH_2 + H$ and $C_6H_6 + C_2H_3 \leftrightarrow C_6H_5CHCH_2 + H$.

The proposed pathways of PAH growth in literature were mainly in two categories: (1) the hydrogen-abstraction-carbon-addition (HACA) mechanism [35-37] including addition of acetylene, ethylene, vinylacetylene, and their radicals on PAH precursors; and (2) the addition of odd carbon radical such as C3 or C5 resonantly stabilized radicals on PAH precursors [38,39]. Since phenyl and benzyl radicals were not detected in this study, we reasonably suppose their concentrations to scale with those of benzene and toluene. Li et al. [40] concluded in their investigation of premixed toluene flames that benzyl radical plays a significant role in PAH formation. However, since the mole fraction of benzene is about nine times of that of toluene in this study, it suggests that this path in diffusion flames may be different from that observed by Li et al. in the low-pressure premixed flames. Aromatics will mainly grow from the reaction of the addition of free radical to benzene. Indene can be formed via the addition of propargyl radical to phenyl ($C_6H_5 + C_3H_3 \leftrightarrow C_9H_8$ (indene)), while the reaction between benzyl and acetylene ($C_6H_5CH_2 + C_2H_2 \leftrightarrow C_9H_8$ (indene) + H) serves a complementary channel [40,41]. In the formation of naphthalene, the reaction between benzyl and propargyl and the addition of ethenyl on phenylacetylene may be important, since the mole fractions of benzene, allene, ethylene, and phenylacetylene seem substantial. For larger aromatics (acenaphthylene, phenanthrene, and pyrene), their formation pathways are too complex to be

predicted just relied on the experimental data in this study. Further modeling study is needed to find out the exact reaction sequences of PAH formation.

Overall, the above results show that C3 species play an important role in benzene and PAH formation process. They promote benzene formation through the C_3H_3 + C_3H_4 reactions and consequently PAH formation through the additions of C2 and C3 species to benzyl or phenyl radicals. The lowest mole fractions of C3 series, benzene, and toluene appear in the 1-butanol flame, while the highest in the *tert*-butanol flame. Therefore, the 1-butanol doped methane/air diffusion flame has the lowest concentration of PAHs, while the *tert*-butanol doped flame has the highest.

4. Conclusions

An experimental study of laminar coflow non-premixed methane/air flames doped with four isomeric butanols has been performed with SVUV-PIMS. Flame species, particularly isomers of benzene precursors and PAHs, have been identified. The quantitative information of species suggests that the dominant benzene formation pathway is the addition of propargyl radical on allene and propyne for all investigated flames. However, the contribution ratios of this pathway are quite different among the four isomeric butanol dopants due to the variant molecular structures. Comparing the productivities of C2-C4 hydrocarbons among the four studied flames, the 1-butanol doped methane flame which produces the most C2 hydrocarbons yields benzene in the least. Therefore, it is concluded that C2 hydrocarbons are not the limiting factor of benzene formation in the butanol flames. Mole fraction data of aromatics presented in this study validates the importance of benzyl and phenyl in the growth of PAHs. However, detailed mechanism on the growth and formation of larger PAHs need to be further developed in the future. The 1-butanol doped methane flame produces the lowest concentrations of aromatics among four isomers, suggesting that it is the most suitable biofuel surrogate of gasoline for cleaner combustion in the near future. The mole fraction data of intermediate species would be of great help in the kinetic modeling of aromatics formation in alcohol combustion.

Acknowledgements

Authors are grateful for the funding support from National Basic Research Program of China (973 Program) (2012CB719701), Natural Science Foundation of China (50925623), and Chinese

Academy of Sciences.

References

[1] K. Kohse-Höinghaus, P. Oßwald, T.A. Cool, T. Kasper, N. Hansen, F. Qi, C.K. Westbrook, P.R. Westmoreland, Angew. Chem. Int. Ed. 49 (2010) 3572-3597.

[2] J.T. Moss, A.M. Berkowitz, M.A. Oehlschlaeger, J. Biet, V. Warth, P.A. Glaude, F. Battin-Leclerc, J. Phys. Chem. A 112 (2008) 10843-10855.

[3] A.L. Demain, J. Ind. Microbiol. Biotechnol. 36 (2009) 319-332.

[4] S. Szwaja, J.D. Naber, Fuel 89 (2010) 1573-1582.

[5] G. Hess, Chem. Eng. News 84 (2006) 9.

[6] G. Hess, Chem. Eng. News 85 (2007) 8.

[7] F.N. Alasfour, Appl. Thermal Eng. 17 (1997) 537-549.

[8] F.N. Alasfour, Int. J. Energy Res. 21 (1997) 21-30.

[9] Y. Yacoub, R. Bata, M. Gautam, Proc. Inst. Mech. Eng., Part A 212 (1998) 363-379.

[10] M. Gautam, D.W. Martin, Proc. Inst. Mech. Eng., Part A 214 (2000) 497-511.

[11] M. Gautam, D.W. Martin, D. Carder, Proc. Inst. Mech. Eng., Part A 214 (2000) 165-182.

[12] T.K. Bhattacharya, S. Chatterjee, T.N. Mishra, Appl. Eng. Agric 20 (2004) 253-257.

[13] G. Black, H.J. Curran, S. Pichon, J.M. Simmie, V. Zhukov, Combust. Flame 157 (2010) 363-373.

[14] K.E. Noorani, B. Akih-Kumgeh, J.M. Bergthorson, Energ. Fuels 24 (2010) 5834-5843.

[15] K.A. Heufer, R.X. Fernandes, H. Olivier, J. Beeckmann, O. Röhl, N. Peters, Proc. Combust. Inst. 33 (2011) 359-366.

[16] S. Vranckx, K.A. Heufer, C. Lee, H. Olivier, L. Schill, W.A. Kopp, K. Leonhard, C.A. Taatjes, R.X. Fernandes, Combust. Flame 158 (2011) 1444-1455.

[17] M.R. Harper, K.M. Van Geem, S.P. Pyl, G.B. Marin, W.H. Green, Combust. Flame 158 (2011) 16-41.

[18] T.S. Norton, F.L. Dryer, Proc. Combust. Inst. 23 (1991) 179-185.

[19] P. Dagaut, S.M. Sarathy, M.J. Thomson, Proc. Combust. Inst. 32 (2009) 229-237.

[20] P. Dagaut, C. Togbé, Fuel 87 (2008) 3313-3321.

[21] P. Dagaut, C. Togbé, Energ. Fuels 23 (2009) 3527-3535.

[22] S.M. Sarathy, M.J. Thomson, C. Togbé, P. Dagaut, F. Halter, C. Mounaim-Rousselle, Combust. Flame 156 (2009) 852-864.

[23] C. Togbé, A. Mze-Ahmed, P. Dagaut, Energ. Fuels 24 (2010) 5244-5256.

[24] C.S. McEnally, L.D. Pfefferle, Proc. Combust. Inst. 30 (2005) 1363-1370.

[25] P. Oßwald, H. Güldenberg, K. Kohse-Höinghaus, B. Yang, T. Yuan, F. Qi, Combust. Flame 158 (2011) 2-15.

[26] B. Yang, P. Oßwald, Y. Li, J. Wang, L. Wei, Z. Tian, F. Qi, K. Kohse-Höinghaus, Combust. Flame 148 (2007) 198-209.

[27] R. Grana, A. Frassoldati, T. Faravelli, U. Niemann, E. Ranzi, R. Seiser, R. Cattolica, K. Seshadri, Combust. Flame 157 (2010) 2137-2154.

[28] P.S. Veloo, F.N. Egolfopoulos, Proc. Combust. Inst. 33 (2011) 987-993.

[29] Y. Li, L. Wei, Z. Tian, B. Yang, J. Wang, T. Zhang, F. Qi, Combust. Flame 152 (2008) 336-359.

[30] J.H. Kent, Combust. Flame 14 (1970) 279-281.

[31] T.A. Cool, K. Nakajima, C.A. Taatjes, A. Mcllroy, P.R. Westmoreland, M.E. Law, A. Morel, Proc. Combust. Inst. 30 (2005) 1681-1688.

[32] J.A. Barnard, Trans. Faraday Soc. 53 (1957) 1423-1430.

[33] Y. Zhang, J. Cai, L. Zhao, J. Yang, H. Jin, Z. Cheng, Y. Li, L. Zhang, F. Qi, Combust. Flame (2011) (in press, doi: 10.1016/j.combustflame.2011.09.005)

[34] K. Yasunaga, Y. Kuraguchi, R. Ikeuchi, H. Masaoka, O. Takahashi, T. Koike, Y. Hidaka, Proc. Combust. Inst. 32 (2009) 453-460.

[35] M. Frenklach, H. Wang, Proc. Combust. Inst. 23 (1991) 1559-1566.

[36] H. Wang, M. Frenklach, J. Phys. Chem. 98 (1994) 11465-11489.

[37] H. Wang, M. Frenklach, Combust. Flame 110 (1997) 173-221.

[38] C.F. Melius, M.E. Colvin, N.M. Marinov, W.J. Pit, S.M. Senkan, Proc. Combust. Inst. 26 (1996) 685-692.

[39] M.B. Colket, D.J. Seery, Proc. Combust. Inst. 25 (1994) 883-892.

[40] Y. Li, J. Cai, L. Zhang, T. Yuan, K. Zhang, F. Qi, Proc. Combust. Inst. 33 (2011) 593-600.

[41] L. Zhang, J. Cai, T. Zhang, F. Qi, Combust. Flame 157 (2010) 1686-1697.

Table 1 Experimental conditions of co-flow diffusion butanol doped methane flames (Unit: SCCM)

	Q_{air}	Q_{Ar}	Q_{N2}	Q_{CH4}	Q_{C4H9OH}
1-butanol	80,000	5.87	438	160	24.5
2-butanol	80,000	5.87	438	160	24.5
iso-butanol	80,000	5.87	438	160	24.5
tert-butanol	80,000	5.87	438	160	24.5

Note: Q_i is the flowrate of species i.

Fig. 1

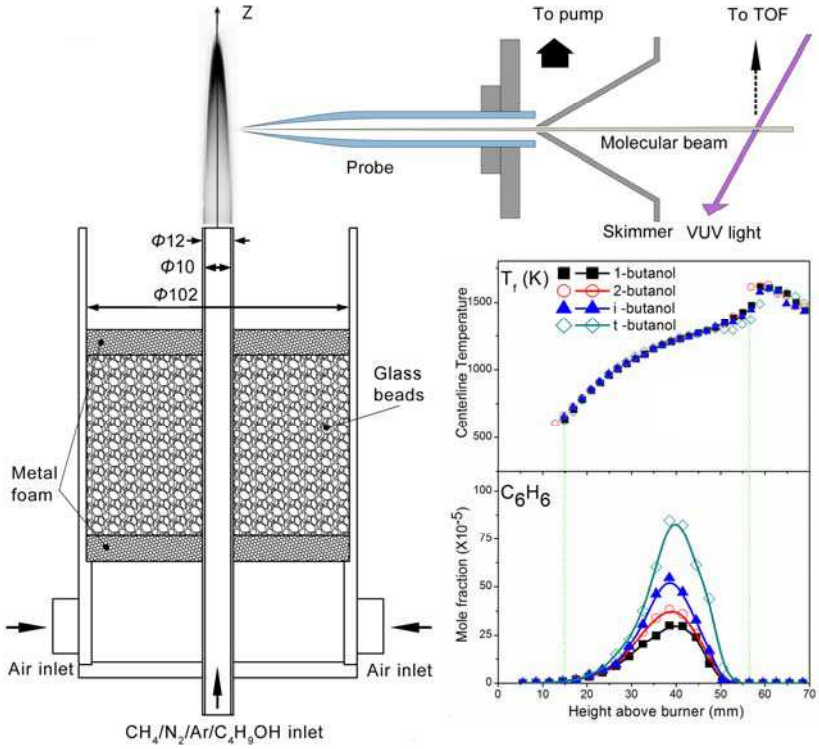

Fig. 1 The left part is a schematic sketch of the burner. The top right is the schematic diagram of co-flow flame analysis apparatus. The bottom right shows the centerline profiles of gas temperature and C_6H_6 (benzene) mole fraction measured in the flames doped with four butanol isomers.

Fig. 2

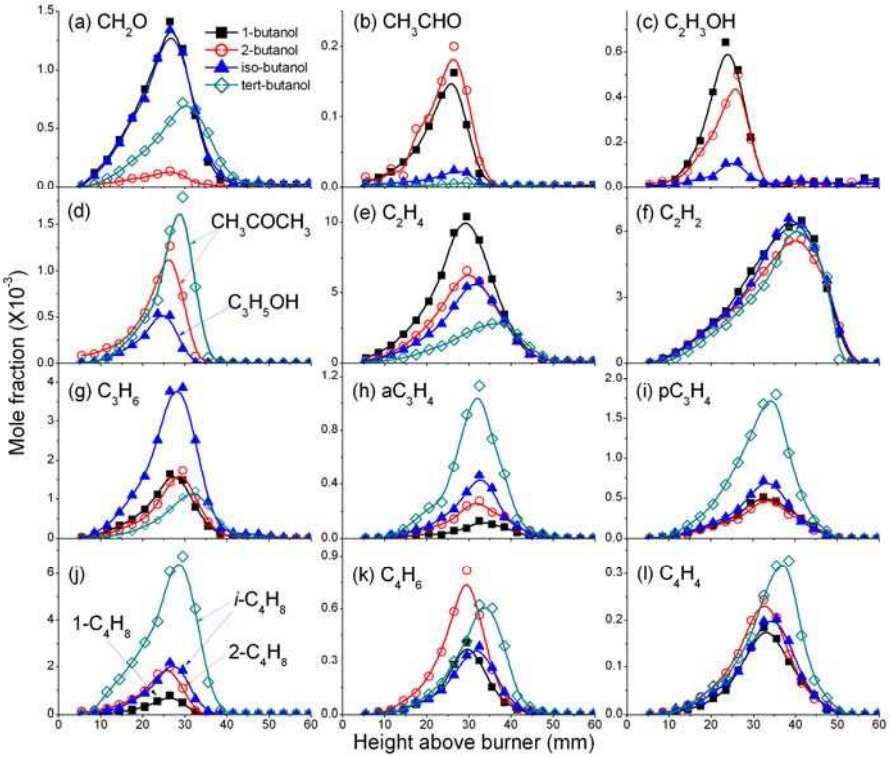

Fig. 2 Measured mole fraction profiles of (a) formaldehyde, (b) acetaldehyde, (c) ethenol, (d) propenol & acetone, (e) ethylene, (f) acetylene, vinylacetylene, (g) propene, (h) allene, (i) propyne (j) butene, (k) 1,3-butadiene, and (l) vinylacetylene in all four butanol doped flames.

Fig. 3

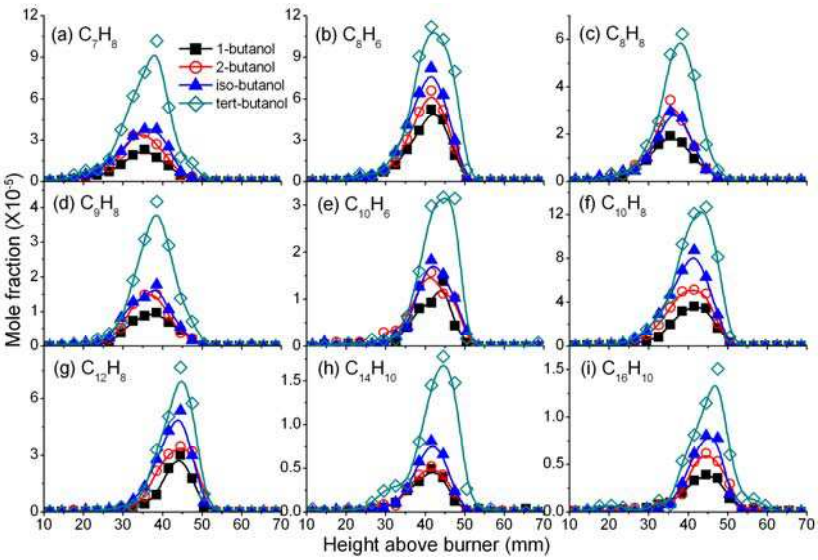

Fig. 3 Measured mole fraction profiles of (a) toluene, (b) phenylacetylene, (c) styrene, (d) indene, (e) 1,4-diethynylbenzene (f) naphthalene, (g) acenaphthylene, (h) phenanthrene, and (i) pyrene in all four butanol doped flames.

Figure Captions

(Color figures in electronic version only)

Fig. 1 The left part is a schematic sketch of the burner. The top right is the schematic diagram of co-flow flame analysis apparatus. The bottom right shows the centerline profiles of gas temperature and C_6H_6 (benzene) mole fraction measured in the flames doped with four butanol isomers.

Fig. 2 Measured mole fraction profiles of (a) formaldehyde, (b) acetaldehyde, (c) ethenol, (d) propenol & acetone, (e) ethylene, (f) acetylene, vinylacetylene, (g) propene, (h) allene, (i) propyne (j) butene, (k) 1,3-butadiene, and (l) vinylacetylene in all four butanol doped flames.

Fig. 3 Measured mole fraction profiles of (a) toluene, (b) phenylacetylene, (c) styrene, (d) indene, (e) 1,4-diethynylbenzene (f) naphthalene, (g) acenaphthylene, (h) phenanthrene, and (i) pyrene in all four butanol doped flames.